Simultaneous fast measurement of circuit dynamics at multiple sites across the mammalian brain

Christina K Kim[1,8], Samuel J Yang[2,8], Nandini Pichamoorthy[3], Noah P Young[3], Isaac Kauvar[2], Joshua H Jennings[3], Talia N Lerner[3], Andre Berndt[3], Soo Yeun Lee[3], Charu Ramakrishnan[3], Thomas J Davidson[3], Masatoshi Inoue[4,5], Haruhiko Bito[4,5] & Karl Deisseroth[3,6,7]

Real-time activity measurements from multiple specific cell populations and projections are likely to be important for understanding the brain as a dynamical system. Here we developed frame-projected independent-fiber photometry (FIP), which we used to record fluorescence activity signals from many brain regions simultaneously in freely behaving mice. We explored the versatility of the FIP microscope by quantifying real-time activity relationships among many brain regions during social behavior, simultaneously recording activity along multiple axonal pathways during sensory experience, performing simultaneous two-color activity recording, and applying optical perturbation tuned to elicit dynamics that match naturally occurring patterns observed during behavior.

Multi-unit electrical recordings from single brain regions have shown that aspects of sensation, cognition and action can be encoded not only in the mean spike rates of individual neurons but also in real-time joint statistical relationships among activity patterns of distinct neural elements. If this principle extends to brain-wide analysis, measurement of neural signals from multiple brain regions, cell types and projection pathways may be required for full elucidation of the mechanisms by which circuit activity patterns represent behavior. Recent technological advances with genetically encoded Ca^{2+} indicators[1–3] (GECIs) have enabled *in vivo* high-resolution cellular imaging of defined neural populations within one to two fields of view[4]; however, these existing approaches typically require head-fixed preparations or are not readily scalable to many regions owing to the size and/or weight constraints of head-mounted microscopes[5] and fiber bundles[6,7].

An alternative method for recording genetically defined activity in freely moving animals, fiber photometry, measures cell population– or projection-defined activity signals through a brain-implanted optical fiber[8–13]. The lightweight and flexible instrumentation of fiber photometry could in principle enable researchers to record from multiple regions simultaneously; however, previous implementations have coupled GECI emission from only one fiber position to a paired and dedicated photodetector. Here we report the design and implementation of the FIP microscope that projects activity signals from many distant, deep brain regions onto each frame of a fast sCMOS (scientific complementary metal-oxide semiconductor) camera. The use of a single camera sensor instead of multiple photodetectors makes this approach scalable to many regions while allowing for the concurrent acquisition of Ca^{2+}-independent emissions as reference signals to control for motion-related artifacts.

We first confirmed that the sCMOS camera could measure GCaMP6f activity *in vivo* with sensitivity comparable to that of existing photoreceiver and lock-in amplifier designs[11] (**Supplementary Note 1** and **Supplementary Fig. 1**). Next, to simultaneously acquire both GECI and control signals, we implemented time-division multiplexing wherein we alternately acquired camera frames with either the optimal Ca^{2+}-dependent excitation wavelength (470 nm for GCaMP6 and 560 nm for R-CaMP2) or the Ca^{2+}-independent isosbestic wavelength[1,3] (410 nm) of the GECI. We confirmed the isosbestic wavelengths of GCaMP6m and R-CaMP2 using simultaneous imaging paired with intracellular current injection-driven defined spiking in cultured neurons (**Supplementary Note 2** and **Supplementary Fig. 2**). Thus we assumed it was likely that any changes observed during excitation of GCaMP6 or R-CaMP2 at 410 nm were due to motion-related artifacts or otherwise unrelated to neural activity and could be removed from Ca^{2+}-dependent activity signals (**Supplementary Fig. 3**).

We then tested the FIP microscope's ability to simultaneously record GCaMP6f Ca^{2+} signals from multiple fibers *in vivo*. A seven-fiber patchcord, tightly bundled on one end and split into seven branches on the other, both delivered excitation and collected emitted light. Each fiber branch was coupled to a fiber optic interface implanted into different, widely dispersed regions in an adult mouse; the sCMOS camera imaged the bundled end, simultaneously measuring fluorescence emission from all seven fibers (**Fig. 1a**). We then measured simultaneous and temporally registered GCaMP6f signals across the brain in a freely moving

[1]Neurosciences Program, Stanford University, Stanford, California, USA. [2]Department of Electrical Engineering, Stanford University, Stanford, California, USA. [3]Department of Bioengineering, Stanford University, Stanford, California, USA. [4]Department of Neurochemistry, Graduate School of Medicine, University of Tokyo, Tokyo, Japan. [5]Core Research for Evolutional Science and Technology, Japan Agency for Medical Research and Development, Tokyo, Japan. [6]Howard Hughes Medical Institute, Stanford University, Stanford, California, USA. [7]Department of Psychiatry and Behavioral Sciences, Stanford University, Stanford, California, USA. [8]These authors contributed equally to this work. Correspondence should be addressed to K.D. (deissero@stanford.edu).

Figure 1 | Simultaneous Ca²⁺ measurements from multiple deep brain regions. (**a**) Schematic of the microscope used for simultaneous FIP Ca²⁺ recordings. The diagram at the lower left shows the time-division multiplexing scheme for simultaneous imaging of GCaMP6 at 470 nm and 410 nm. (**b**) Left, schematic of fiber placements in seven different brain regions expressing GCaMP6f. Right, example Ca²⁺ traces and simultaneously recorded control traces from a freely moving mouse. (**c**) GCaMP6f fluorescence traces simultaneously acquired across seven brain regions of a mouse when it was alone or socializing with a novel mouse. (**d**) Top, heat maps of Pearson's correlation coefficient (*r*) calculated between brain regions for the mouse represented in **c**. Bottom, spatial representations of *r* between different brain regions. (**e**) The mean *r* value between all brain regions in mice alone (0.31 ± 0.024) and in mice socializing with a novel mouse (0.43 ± 0.024). Data plotted as mean ± s.e.m. ***$P < 0.001$, Wilcoxon's rank-sum test; $n = 84$ pairs, 4 mice. (**f**) Schematic of surgery and recording setup for VTA-DA projection imaging. (**g**) GCaMP6f fluorescence traces simultaneously acquired in each brain region of a mouse in response to reward and tail shock. Data plotted as mean (dark green curves) ± s.e.m. (light green shaded regions). Gray bars indicate time of reward or shock. (**h**) Responses to reward and shock in each brain region ($dF/F_{stimulus} − dF/F_{baseline}$) for the mouse represented in **g**. Data plotted as mean and s.e.m. *$P < 0.05$, Wilcoxon's signed-rank test; $n = 6$ trials, 1 mouse. LH, lateral hypothalamus; BNST, bed nucleus of stria terminalis; Norm, normalized.
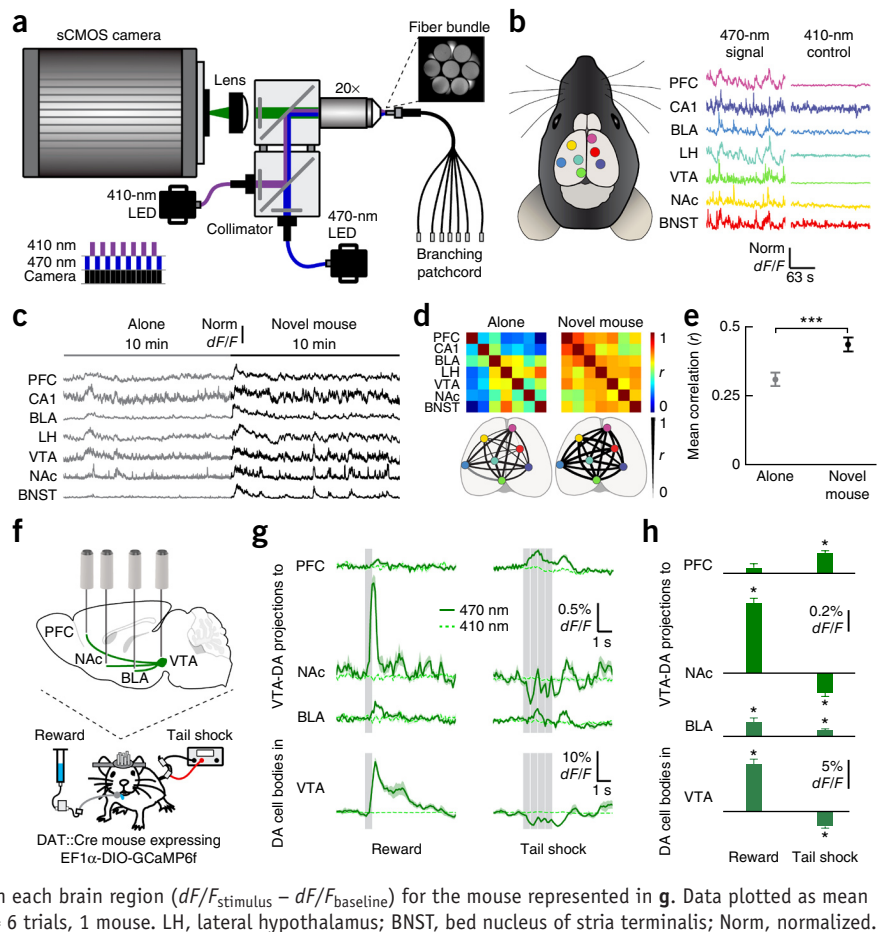
mouse (**Fig. 1b** and **Supplementary Note 3**). We recorded from dopaminergic (DA) neurons in the ventral tegmental area (VTA) and from CaMKIIα-expressing neurons in the bed nucleus of the stria terminalis, nucleus accumbens (NAc), lateral hypothalamus, basolateral amygdala (BLA), hippocampal region CA1 and prefrontal cortex (PFC). GCaMP6f fluorescence signals were robust with 470-nm excitation but not with 410-nm excitation, with which only small, non–Ca²⁺-dependent changes were observed (**Fig. 1b**). We then recorded neural activity across all seven brain regions during naturalistic social interactions in freely moving mice (**Supplementary Video 1**) and normalized 470-nm signals to 410-nm controls. Spontaneous activity could be robustly observed in all regions, in addition to time-locked increases in fluorescence activity after the introduction of a novel mouse (**Fig. 1c**). We calculated Pearson's correlation coefficient *r* among brain regions when a mouse was alone or interacting with a novel mouse and observed global increases in *r* during socializing (**Fig. 1d,e**). Shuffling analysis confirmed that this increase was significantly greater than would be expected from simple increased activity in all regions ($P < 0.001$, 1,000 shuffle permutation test; Online Methods).

We next tested system sensitivity limits by recording Ca²⁺ signals not only from populations of cell bodies but also from axonal projections to multiple independent regions. We expressed Cre-dependent GCaMP6f in the VTA of DAT∷Cre driver mice[14] and implanted optical fibers in the PFC, NAc, BLA and VTA to simultaneously record from VTA-DA cell bodies and their downstream axonal terminals while administering time-locked water rewards

or aversive tail shocks (**Fig. 1f**). We found that VTA-DA cell bodies exhibited increased activity during reward and decreased activity during shock, consistent with previous recordings from VTA-DA neurons[15–17]. In contrast, activity in the VTA-DA→BLA projection increased during both reward and shock. The VTA-DA→NAc projection showed a pattern similar to that of VTA-DA cell bodies, but activity in VTA-DA→PFC projections exhibited yet a third pattern (increased response to shock but not reward; **Fig. 1g,h**). Supporting the validity of the FIP approach, these results were consistent with previous studies that individually tracked activity in different populations of VTA-DA neurons encoding rewarding or aversive stimuli depending on the projection target[18,19] (though without the joint simultaneity of FIP during behavior). Raw GCaMP6f fluorescence traces are shown in **Supplementary Figure 4a,b**, and control signals are summarized in **Supplementary Figure 4c**. Example videos of multiple GCaMP6f emissions during reward and shock are shown in **Supplementary Videos 2** and **3**, and **Supplementary Table 1** summarizes the reproducibility of significant GCaMP6f responses recorded during reward and shock. Histology confirmed the locations of fibers and the expression of GCaMP6f in cell bodies and terminals (**Supplementary Fig. 5**).

We next found that the FIP microscope was readily adaptable for dual-color imaging of different populations using two different Ca²⁺ sensors measured through the same fiber (**Supplementary Fig. 6**). We labeled DA and non-DA VTA neurons in DAT∷Cre mice using a Cre-activated (DIO) R-CaMP2 virus and a Cre-deactivated

Figure 2 | Dual-color imaging of different populations and simultaneous recording and perturbation of neural activity. (**a**) Schematic of dual-color imaging surgery. (**b**) Histology confirming non-overlapping labeled populations of VTA-DA and VTA–non-DA neurons. Scale bar, 25 μm. (**c**) VTA-DA and VTA–non-DA fluorescence traces acquired after reward or tail shock. Data plotted as mean (curves) ± s.e.m. (shading around curves). Gray bars indicate time of reward or shock. (**d**) Mean responses to reward and shock ($dF/F_{stimulus} − dF/F_{baseline}$) for the mouse represented in **c**. Data plotted as mean and s.e.m. VTA-DA activity increased in response to reward (5.39% ± 0.32% dF/F) and decreased in response to shock (−1.18% ± 0.45% dF/F), whereas VTA–non-DA activity increased after both reward (3.26% ± 0.14% dF/F) and shock (2.08% ± 0.14% dF/F). *$P < 0.05$, Wilcoxon's signed-rank test; $n = 10$ trials, 1 mouse. (**e**) Schematic of combined imaging and optogenetics surgery. (**f**) Schematic of imaging paradigm. (**g**) GCaMP6f

fluorescence in response to 5 μW of 470-nm stimulation, 594-nm stimulation (different shades of orange from light to dark denote 0.5 mW, 1 mW and 2 mW of power, respectively) or reward. Gray bar indicates time of stimulation. (**h**) Mean response to bReaChES stimulation and reward ($dF/F_{stimulus} − dF/F_{baseline}$). Data plotted as mean ± s.e.m. Color-coding matches the key in **g**. The mean response to 470-nm cross-stimulation (2.27% ± 0.57% dF/F) was significantly smaller than the response to reward (8.27% ± 1.63% dF/F) (*$P < 0.05$, Wilcoxon's rank-sum test, $n = 6$ trials for 470 nm and 4 trials for reward/1 mouse). Dashed lines indicate ±s.e.m. Stim, stimulus.
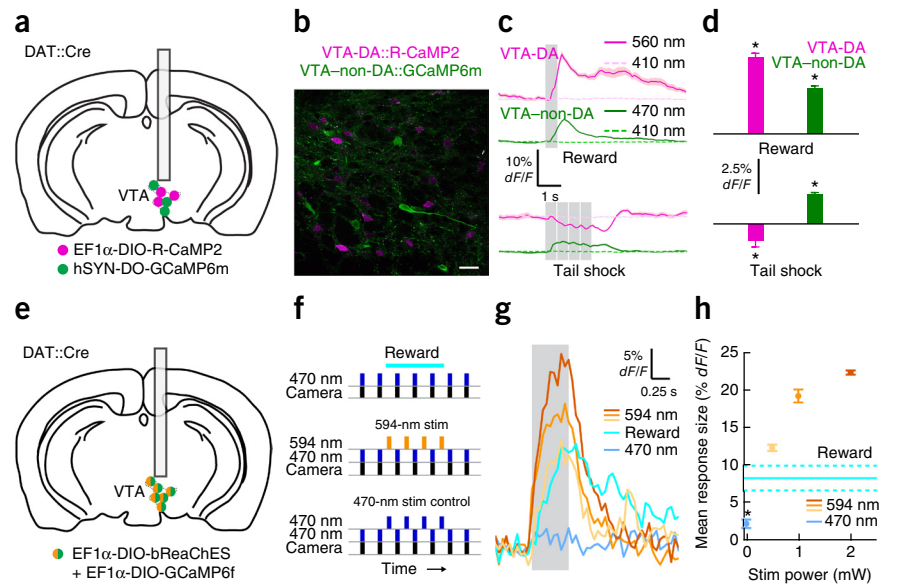
(DO) GCaMP6m virus, respectively (**Fig. 2a**). This viral strategy resulted in labeling of largely non-overlapping populations of R-CaMP2 and GCaMP6m neurons in VTA (**Fig. 2b**), and expression of DIO-R-CaMP2 colocalized with tyrosine hydroxylase staining for DA neurons (**Supplementary Fig. 7**). While monitoring these neural populations with FIP, we administered reward or tail shock stimuli. Confirming the results in **Figure 1g,h**, VTA-DA activity measured with R-CaMP2 significantly increased during reward and significantly decreased during shock (**Fig. 2c,d**), whereas VTA–non-DA activity significantly increased during both reward and shock (**Fig. 2c,d**), consistent with previous electrical recordings[17]. There was no significant change in R-CaMP2 or GCaMP6m control fluorescence with 410-nm excitation during reward or shock (data not shown; $P > 0.05$, Wilcoxon's signed-rank test; $n = 10$ trials with one mouse).

Finally, we found that FIP readily allowed tuning of optogenetic stimulation to match naturally occurring activity levels in the very same targeted neural population of the same subject, a long-sought fundamental goal in optogenetics. We began with simultaneous recording and perturbation of activity[20] using GCaMP6f and a potent, fast red-shifted channelrhodopsin, bReaChES (Online Methods, **Supplementary Note 4** and **Supplementary Fig. 8**). We incorporated a 594-nm laser for bReaChES stimulation (**Supplementary Fig. 9**) and coexpressed DIO-bReaChES and DIO-GCaMP6f in the VTA of DAT∷Cre mice to image and perturb VTA-DA neurons (**Fig. 2e**). We anticipated that FIP's high sensitivity would allow recording of GCaMP6f with very low-power 470-nm excitation to minimize unwanted cross-stimulation of bReaChES (**Supplementary Note 5**). To quantify cross-stimulation, we measured GCaMP6f responses to additional interleaved pulse trains of 470-nm light mimicking the imaging light; we also measured GCaMP6f responses to 594-nm pulses and to a naturalistic water reward (**Fig. 2f**). Minimal

changes in GCaMP6f fluorescence resulted from 5 μW of 470-nm imaging light measured at the patchcord face (**Fig. 2g**); larger GCaMP6f changes indicative of opsin cross-stimulation were seen at higher light powers (**Supplementary Fig. 10a,b**). Crucially, 5 μW of 470-nm imaging light was sufficient for measurement of VTA-DA responses to 594-nm bReaChES stimulation, allowing tuning of optogenetic response sizes to match amplitudes of naturalistic VTA-DA responses to reward in the same animal (**Fig. 2g,h**). A control DAT∷Cre mouse coexpressing DIO-GCaMP6f and DIO-mCherry exhibited no GCaMP6f responses to interleaved 470-nm or 594-nm stimulation light, although it did exhibit GCaMP6f transients as expected during interaction with a novel mouse[11] (**Supplementary Fig. 10c,d**).

Future FIP developments may include extension of dual-color imaging and optogenetic perturbation across all fibers in the interface, as well as the adaptation of faster and more sensitive cameras for newer probes such as genetically encoded voltage sensors. FIP microscopy already enables simultaneous parallel measurements of Ca²⁺ activity in multiple distant brain regions or axonal projection pathways, and it also allows simultaneous dual-color imaging through a single fiber at any one region. Finally, FIP enables simultaneous optogenetic stimulation and activity readout of the same population in a given animal, either during the optogenetic stimulation itself or during naturalistic behavior. The latter behavioral capability serves the dual purpose of allowing more finely tuned optogenetic manipulations that mimic physiological responses of neurons *in vivo* and opening the door to closed-loop control using waveforms and activity patterns that are adjusted in real time to test models of the underlying neural system.

METHODS

Methods and any associated references are available in the online version of the paper.

Accession codes. GenBank: bReaChES, KU559019.

Note: Any Supplementary Information and Source Data files are available in the online version of the paper.

AUTHOR CONTRIBUTIONS

C.K.K., S.J.Y. and K.D. designed the experiments and wrote the paper with comments from all other authors. C.K.K., S.J.Y. and I.K. designed the FIP microscope. C.K.K. and S.J.Y. built the FIP microscope. N.P.Y. and S.J.Y. wrote software for image acquisition. C.K.K. built the head-fixed behavioral apparatus and wrote software for stimulus delivery. C.K.K. and S.J.Y. performed simultaneous photoreceiver and sCMOS measurements. C.K.K., N.P. and J.H.J. performed surgeries and behavioral experiments. C.K.K., S.J.Y. and I.K. performed simultaneous stimulation and imaging experiments. T.N.L. performed the GECI isosbestic cell culture experiments. A.B., S.Y.L. and C.R. designed and characterized the bReaChES construct. C.R. designed and generated constructs for viruses and generated transfected cultured neurons. T.J.D. contributed to photoreceiver setup design and isosbestic control design. M.I. and H.B. provided the R-CaMP2 construct. C.K.K. analyzed all data. K.D. supervised all aspects of the project.

1. Tian, L. *et al. Nat. Methods* **6**, 875–881 (2009).
2. Chen, T.-W. *et al. Nature* **499**, 295–300 (2013).
3. Inoue, M. *et al. Nat. Methods* **12**, 64–70 (2015).
4. Lecoq, J. *et al. Nat. Neurosci.* **17**, 1825–1829 (2014).
5. Ghosh, K.K. *et al. Nat. Methods* **8**, 871–878 (2011).
6. Flusberg, B.A. *et al. Nat. Methods* **5**, 935–938 (2008).
7. Szabo, V., Ventalon, C., De Sars, V., Bradley, J. & Emiliani, V. *Neuron* **84**, 1157–1169 (2014).
8. Lütcke, H. *et al. Front. Neural Circuits* **4**, 9 (2010).
9. Schulz, K. *et al. Nat. Methods* **9**, 597–602 (2012).
10. Cui, G. *et al. Nature* **494**, 238–242 (2013).
11. Gunaydin, L.A. *et al. Cell* **157**, 1535–1551 (2014).
12. Cui, G. *et al. Nat. Protoc.* **9**, 1213–1228 (2014).
13. Lerner, T.N. *et al. Cell* **162**, 635–647 (2015).
14. Bäckman, C.M. *et al. Genesis* **44**, 383–390 (2006).
15. Schultz, W. *J. Neurophysiol.* **80**, 1–27 (1998).
16. Ungless, M.A., Magill, P.J. & Bolam, J.P. *Science* **303**, 2040–2042 (2004).
17. Cohen, J.Y., Haesler, S., Vong, L., Lowell, B.B. & Uchida, N. *Nature* **482**, 85–88 (2012).
18. Lammel, S., Ion, D.I., Roeper, J. & Malenka, R.C. *Neuron* **70**, 855–862 (2011).
19. Lammel, S. *et al. Nature* **491**, 212–217 (2012).
20. Grosenick, L., Marshel, J.H. & Deisseroth, K. *Neuron* **86**, 106–139 (2015).

ONLINE METHODS

Core FIP setup and modifications. The main FIP platform consists of a wide-field microscope capable of imaging a bundle of one or more (up to seven in our case) fiber faces, with a series of dichroic mirrors integrated into the microscope to simultaneously couple in excitation light sources of various wavelengths. Custom MATLAB (Mathworks) routines are used to control the timing of the different excitation light sources, to synchronously acquire camera frames and to digitally sum and compute the total fluorescence from each of the fibers in each camera frame in real time. The excitation light sources, dichroics and acquisition-timing protocols can be reconfigured to support the concurrent acquisition of isosbestic control signals, combinations of dual-color recording, and simultaneous recording and stimulation.

Core FIP setup. A custom patchcord of seven bundled 400-µm-diameter 0.48-NA fibers (Doric Lenses) was used to collect fluorescence emission. One end of the patchcord terminated in an SMA connector (Thorlabs, SM1SMA) mounted at the working distance of the objective, and the other end terminated in seven individual 1.25-mm-diameter stainless steel ferrules. These ferrules were coupled via ceramic sleeves (Thorlabs, ADAL1) to 1.25-mm-diameter ferrules implanted into a mouse. The bundled fiber faces were imaged through a 20×/0.75-NA objective (Nikon, CFI Plan Apo Lambda 20×) through a series of reconfigurable dichroic mirrors. Fluorescence emission from the fibers passed through a 535-nm bandpass fluorescence emission filter (selected for GCaMP recording; Semrock, FF01-535/22-25). The fluorescence image was focused onto the sensor of an sCMOS camera (Hamamatsu, ORCA-Flash4.0) through a tube lens (Thorlabs, AC254-035-A-ML). The reconfigurable dichroic mirrors were mounted in removable dichroic cube holders (Thorlabs, DFM1) that enabled two different light sources to be coupled in. In the standard configuration, a 470-nm LED filtered with a 470-nm bandpass filter (Thorlabs, M470F1 and FB470-10) was fiber-coupled into the dichroic cube holder using a 1,000-µm-diameter 0.48-NA fiber (Thorlabs, M71L01) and a 405-nm, $f = 4.02$ mm, 0.6-NA collimator (Thorlabs, F671SMA-405 and AD11F) with a 495-nm longpass dichroic mirror (Semrock, FF495-Di02-25 ×36). This produced an excitation spot of ~2.5-mm diameter (10-mm objective focal length ÷ 4.02-mm collimator focal length × 1,000-µm-diameter fiber) at the working distance of the 20× objective. This spot was sufficiently large to fill all of the fibers of the seven-fiber branching patchcord. Typically the light powers emitted from the different fibers will be within 25–50% of each other. The LEDs were controlled by a driver enabling digital modulation up to 1 kHz (Thorlabs, LEDD1B). **Supplementary Note 6** describes additional system design, alignment and calibration considerations.

Modifications for sCMOS and lock-in amplifier photoreceiver comparison. In order to precisely replicate the previous photoreceiver lock-in detection approach using a single 400-µm, 0.48-NA imaging patchcord, we introduced an optical chopping wheel after the collimated 470-nm LED (Thorlabs, MC1510 and MC2000). We coupled the LED to the microscope via a 200-µm-diameter, 0.39-NA fiber (Thorlabs, M75L01) and a 543-nm, $f = 7.86$ mm, 0.51-NA collimator (Thorlabs, F240FC-A and AD12F) to illuminate only the center ~254-µm-diameter region of the 400-µm-diameter patchcord (10-mm objective focal length ÷ 7.86-mm collimator focal length × 200-µm-diameter fiber). We achieved

this alignment by positioning the collimator using a five-axis kinematic mount (Thorlabs, K5X1) and using the camera to visualize both the 400-µm-diameter imaging patchcord and the size of the excitation spot from the 200-µm-diameter fiber-coupled LED using a fluorescent slide (Chroma, 92001) mounted at the working distance of the objective. The filtered GCaMP6 emission was then directed to both the sCMOS and the photoreceiver using a 50:50 beamsplitter (Thorlabs, BSW10R). A 10×/0.45-NA objective (Nikon, CFI Plan Apo Lambda 10×) was used to focus half of the GCaMP emission onto the ~1-mm sensor of the photoreceiver (Newport, 2151), which was mounted on an *x-y-z* translator (Thorlabs, PT1 and PT2). Lastly, the signal from the optical chopping wheel was synchronized to a lock-in amplifier (Stanford Research, SR810 DSP), the output of which was sampled and digitized at 10 kHz using data-acquisition hardware (National Instruments, NI PCIe-6343-X).

Setup for concurrent acquisition of isosbestic control. For measurements of GCaMP6 emission, we used both a 405-nm LED and a 470-nm LED (Thorlabs, M405F1 and M470F1) as excitation sources for the Ca^{2+}-dependent and Ca^{2+}-independent isosbestic control measurements, respectively. The two LEDs were filtered with 410-10–nm and 470-10–nm bandpass filters (Thorlabs, FB410-10 and FB470-10), fiber coupled as described above, combined using a 425-nm longpass dichroic mirror (Thorlabs, DMLP425R) and coupled into the microscope using a 495-nm longpass dichroic mirror (Semrock, FF495-Di02-25 ×36).

Dual-color recording setup. To enable simultaneous GCaMP6 and R-CaMP2 recording, we removed the 535-nm bandpass emission filter and introduced an image splitter (Photometrics, DualView-Lambda) between the camera and the tube lens, which enabled us to record the GCaMP6 and R-CaMP2 emission onto separate halves of the same camera sensor. Inside the image splitter, a 560-nm dichroic mirror (Chroma, T560lpxr-UF2-26 × 28 × 2 mm) separated the emission into two channels, each of which was additionally filtered by a 600-37–nm (Semrock, FF01-600/37-25) and a 520-35–nm emission filter (Semrock, FF01-520/35-25) and then projected onto the camera sensor. An additional dichroic cube allowed us to incorporate a 565-nm LED (Thorlabs, M565F1) for R-CaMP2 excitation with a 560-14–nm excitation filter (Semrock, FF01-560/14-25), in conjunction with the 410-nm and 470-nm LEDs as described previously for GCaMP6 recording. Each of the three LEDs was coupled via a 1,000-µm-diameter, 0.48-NA fiber (Thorlabs) to either a 405-nm, $f = 4.02$ mm, 0.6-NA collimator (410-nm and 470-nm LED: Thorlabs, F671SMA-405 and AD11F) or a 543-nm, $f = 4.34$ mm, 0.57-NA collimator (560-nm LED: Thorlabs, F230SMA-A). The 410-nm and 470-nm output from the collimators were first combined with a 425-nm longpass dichroic mirror (Thorlabs, DMLP425R) and then combined with the 560-nm light using a second 520-nm dichroic (Semrock, FF520-Di02-25 ×36) before finally being coupled into the microscope using a third multiband dichroic (Semrock, FF410/504/582/669-Di01-25 ×36).

Setup for simultaneous recording and stimulation. For combined imaging and optogenetic stimulation, the 565-nm LED used for dual-color recording was replaced with a 594-nm laser (Cobolt, Mambo, 100 mW). The 594-nm laser was filtered with a 590-10–nm bandpass filter (Thorlabs, FB590-10). An additional 525-39–nm GFP emission filter (Semrock, FF01-525/39-25) was placed in front of the tube lens along with a 594-nm notch filter

(Semrock, NF03-594E-25) to minimize direct laser emission detected by the camera. A multiband dichroic (Semrock, Di01-R405/488/594-25 ×36) was used to reflect 470-nm and 594-nm excitation light into the back of the 20× objective. A high-speed shutter (Stanford Research Systems, SR474) modulated the laser in synchrony with the other LEDs and the camera. To enable the delivery of 470-nm excitation light at two different power levels for 470-nm cross-stimulation experiments, we replaced the 594-nm laser with another 470-nm LED and replaced the dichroic combining the 470-nm and 594-nm light with a 50:50 beamsplitter. During the cross-stimulation experiments, one 470-nm LED was set to a lower power and activated for every camera exposure, and the other 470-nm LED was set to a similar or higher power and activated only during the stimulation periods.

Time-division multiplexing. To enable the concurrent recording of multiple channels per fiber (or for simultaneous optogenetic stimulation), we used a time-division multiplexing strategy to time-sequentially sample each channel individually. Schematics of the time-division multiplexing strategy used for each experiment are shown in **Figures 1a** and **2f** and **Supplementary Figure 6**. Briefly, for GCaMP6 imaging, consecutive camera frames were captured using alternating 470-nm and 410-nm excitation sources, such that every other camera frame was captured using either 470-nm or 410-nm light. Thus if the camera was capturing images at 40 Hz, the individual 470-nm and 410-nm signals were sampled at 20 Hz. For simultaneous GCaMP6 and R-CaMP2 imaging, camera frames were captured using either alternating excitation sources of 470 nm and 560 nm or 410 nm alone. For simultaneous GCaMP6 imaging and optogenetic stimulation, camera frames were captured only with 470-nm excitation light, and additional 470-nm or 594-nm stimulation light pulses were independently controlled.

Image acquisition using MATLAB. Although the technique described here could be implemented using the standalone image-acquisition software for the sCMOS camera and digital function generators to control the light sources, we wrote custom MATLAB routines to control all hardware and streamline data acquisition. All software ran on a Dell T5600 computer running Windows 7 (64-bit). A custom MATLAB GUI controlled both the sCMOS camera through the MATLAB Image Acquisition Toolbox and the LED light sources through a data-acquisition device (National Instruments, NI PCIe-6343-X) and the MATLAB Data Acquisition Toolbox. To minimize the raw data volume for real-time applications, we set the camera to 4-by-4 pixel binning and semi-automatically located a subregion containing only fiber ends from which data would be acquired. Using this software, we were able to calculate the seven fiber signals from the raw camera frame within ~2–3 ms (measured when collecting both Ca^{2+} and isosbestic signals at 40 Hz, and given our computer's configurations). Separate scripts for each experiment generated digital control signals to operate any mouse behavior peripheral hardware.

Code availability. All protocols, software and other resources, including our GUI software and example behavior control scripts, are freely available https://github.com/deisseroth-lab/multifiber, http://clarityresourcecenter.org/fiberphotometry.html.

Head-fixed apparatus and stimulus delivery. Except during the free-movement seven-fiber recordings, mice were head-fixed above a running wheel (Ware, small 6-inch wheel) using a custom machined head-plate holder. Custom-written MATLAB scripts delivered digital control signals to trigger water rewards and tail shocks synchronized to the camera imaging. Water rewards were delivered through a small-animal feeding tube (Popper and Sons, 16-gauge) connected to a normally closed solenoid (Valcor, SV74P61T-1). The solenoid was powered by a 12-V DC battery, and the power was gated by a metal-oxide semiconductor field-effect transistor (Mouser Electronics). Tail shocks were administered using a stimulus isolator (WPI, Isostim A320R). The positive and negative leads of the isolator were connected by lead wires (Roscoe Medical, WW3005) to two pre-gelled electrodes (Sonic Technology) that were attached to the mouse's tail.

Analysis. All analysis was performed using custom MATLAB scripts. Regions of interest were first manually drawn around the fiber(s) on the basis of a mean image of the movie. The average fluorescence intensity was calculated for each fiber. We acquired a 'dark frame' image by taking a movie with the patchcord attached to the mouse, but with no LEDs on, to account for extraneous, non–GECI-related light contributing to the signal. We subtracted this offset from the fluorescence intensity for each fiber. We then fit a double exponential to a thresholded version of the fluorescence time series and subtracted the best fit from the unthresholded signal to account for slow bleaching artifacts. We calculated a single baseline fluorescence value, either as the median of the entire trace (which robustly estimated the baseline fluorescence) or by manually defining the baseline during visually identified periods of rest. We calculated the normalized change in fluorescence (dF/F) by subtracting the baseline fluorescence from the fiber fluorescence at each time point and dividing that value by the baseline fluorescence. For seven-fiber experiments, we further normalized the dF/F by the maximum value for each fiber. For the analysis shown in **Figure 1c–e**, we scaled the 410-nm reference trace to best fit the 470-nm signal using least-squares regression[13]. We then subtracted the scaled 410-nm reference trace from the 470-nm signal to obtain the motion-corrected 470-nm signal. Other than that done for the plots shown in **Figure 1b** for the seven-fiber imaging, no additional smoothing or filtering was applied to fluorescence measurements. For **Figure 1b**, a 1-s average sliding window was applied to the traces. To calculate correlation coefficients, we used MATLAB's "corr" function. To ensure that the increase in correlation during social interactions was significantly greater than what one would expect from merely increased activity, we circularly permuted each fiber's trace 1,000 times using a random shift between 0 and 5 min. For each shuffle, we calculated the pooled mean r value across all mice and unique brain region pairs. Here a P value of <0.001 means that none of the mean r values calculated from the 1,000 shuffled traces was greater than the actual calculated mean r value. For all statistical tests, nonparametric tests were used. Specific details of tests used can be found in figure legends. We ensured that the variance between data used for comparisons was similar.

Experimental parameters. To ensure reproducibility, we collected a minimum of four (typically six) repeated trials per animal in experiments when feasible and performed all experiments at least twice. The number of mice used in each experiment is presented in the subsections below. Because an internal control

was performed for each animal (410-nm isosbestic control), no randomization was needed to assign animals to different experimental groups. Therefore, experimenters were not blinded to animal identity. No animals were excluded from the study.

sCMOS and lock-in amplifier photoreceiver experiments. Two mice were water deprived to ~80% of their starting weight. Head-fixed mice were trained to lick water rewards that were delivered through a feeding syringe. Water rewards consisted of a 0.25-s opening of the solenoid and were delivered at 10-s intervals. The signal-to-noise ratio was calculated as the peak dF/F divided by the s.d. of the baseline dF/F. Here the peak dF/F was the maximum value during the first 2 s of reward, and the baseline dF/F was measured during the 0.5 s before reward delivery. Recordings were taken from only a single fiber in the VTA. We used a low imaging power of 2.5 µW (measured at the face of a 400-µm-diameter patchcord). Imaging parameters are presented in **Supplementary Note 1**.

Multifiber experiments. For the seven-fiber experiment, four mice were used. Mice were allowed to freely navigate a cage and socialize with a novel mouse (of the same gender and age) while we recorded Ca^{2+} signals. We imaged at 40 Hz with alternating frames of 470-nm and 410-nm excitation wavelengths, resulting in frame rates of 20 Hz for both GCaMP6 Ca^{2+} and isosbestic control signals. For the four-fiber experiments, seven mice were water deprived and administered either water rewards or tail shocks while head-fixed and running on a wheel. Water rewards consisted of a 0.5-s opening of the solenoid, and tail shocks were given as 450-ms pulses spaced 5 ms apart for 2 s (four shocks at 0.5 Hz). Water rewards and shocks were given at 10-s intervals. We defined the response size to reward or shock as the difference between the mean stimulus dF/F during the first 1 s of the reward or shock and the mean baseline dF/F during the 2 s before the reward or shock. We imaged at 20 Hz with alternating pulses of 470-nm and 410-nm excitation wavelengths, resulting in frame rates of 10 Hz for both GCaMP6 Ca^{2+} and isosbestic control signals. Typically we used 10–20 µW of 470-nm imaging light power and adjusted the 410-nm LED light power to approximately match the GCaMP6 fluorescence emission produced by the 470-nm imaging light.

Dual-color experiments. A single mouse was water-deprived and administered either water rewards or tail shocks while head-fixed with the same parameters as in the multifiber experiments. Response sizes to reward and shock were calculated as described for the multifiber experiments. We imaged at 20 Hz with alternating pulses of simultaneous 470-nm and 560-nm light and 410-nm light, resulting in frame rates of 10 Hz for GCaMP6 and R-CaMP2, as well as for the control signals. We used 10–20 µW of 470-nm and 560-nm imaging light power and adjusted the 410-nm LED light power to approximately match the GCaMP6 and R-CaMP2 fluorescence emission produced by the 470-nm and 560-nm imaging light.

Combined imaging and stimulation experiments. Two mice (bReaChES and mCherry control) were water-deprived and administered either optogenetic stimulation or water rewards while head-fixed with the same parameters as in the multifiber experiments. We defined the response size to optogenetic stimulation or reward as the difference between the mean stimulus dF/F during the first 0.5 s of the light or reward and the mean baseline dF/F during the 0.5 s before the light or reward. To sample

Ca^{2+} signals at 20 Hz, we used 470-nm excitation pulses that were 12.5 ms in length and spaced 50 ms apart for a 25% duty cycle. The camera exposed frames only during each 470-nm excitation pulse, resulting in 25% duty cycle imaging. Additional 470-nm or 594-nm stimulation pulses were delivered between the 470-nm imaging excitation pulses at a rate of 20 Hz for 0.5 s (ten pulses with a 12.5-ms pulse width for a 25% duty cycle). Although we could have used longer exposure times to increase the amount of signal we recorded, we chose to have a larger separation between the stimulation periods and the camera exposure times, so that there was no question about whether we were measuring signal artifacts where the 470-nm or 594-nm stimulation pulses contributed additional excitation of GCaMP6 within a camera exposure. We did not record a 410-nm isosbestic GCaMP control signal for these experiments. We used identical light powers for the 470-nm imaging and stimulation pulses for the 5-µW and 10-µW experiments. However, for the 50-µW and 220-µW 470-nm stimulation pulses, we kept the imaging 470-nm LED at 10 µW to avoid unnecessary bleaching of the GCaMP6 fluorescence and set the additional stimulation 470-nm LED to 50 or 220 µW. For all 594-nm stimulation pulses and water-reward measurements, the imaging 470-nm LED was kept at 5 µW. For the control mouse, GCaMP6 fluorescence was recorded with 20-µW pulses of 470-nm imaging light and identical 20-µW pulses of 470-nm stimulation light and 0.5-mW pulses of 594-nm stimulation light. We also recorded GCaMP6 fluorescence with 50-µW pulses of 470-nm imaging light and identical 50-µW pulses of 470-nm stimulation light and 0.5-mW pulses of 594-nm stimulation light.

Cultured neuron intracellular patching and imaging. Dissociated rat hippocampal neurons were cultured and transfected with both GCaMP6m and R-CaMP2 as previously described[13]. Coverslips of cultured neurons were transferred from the culture medium to a recording bath filled with Tyrode's solution (containing (in mM) 125 NaCl, 2 KCl, 2 $CaCl_2$, 2 $MgCl_2$, 30 glucose and 25 HEPES). Whole-cell patch-clamp recordings were performed on healthy GECI-expressing neurons at room temperature. The resistance of the glass patch pipettes was 3–4 MΩ (Sutter Instruments, P-2000) when filled with intracellular solution containing the following (in mM): 150 K-gluconate, 5 NaCl, 1 $MgCl_2$, 0.2 EGTA, 10 HEPES, 2 Mg-ATP and 0.3 Na-GTP, adjusted to pH 7.3 with KOH. Signals were amplified with a Multiclamp 700B amplifier and acquired using a DigiData 1440A digitizer sampled at 10 kHz and filtered at 2 kHz (Molecular Devices). All electrophysiological data acquisition was performed using pCLAMP software (Molecular Devices). Imaging was performed using a 40×/0.8-NA objective (Olympus), Rolera XR camera (Q-Imaging) and Spectra X Light excitation source (Lumencor), all coupled to an Olympus BX51 WI microscope. The following bandpass filters were used with the Lumencor for excitation wavelengths: 405-10 nm (Thorlabs, FB405-10), 470-10 nm (Thorlabs, FB470-10) and 560-10 nm (Thorlabs, FB560-10). GCaMP6m emission was reflected off a 495-nm dichroic mirror (Semrock, FF495-Di03-25 ×36) and passed through a 535-30–nm emission filter (Chroma, ET535/30m), and R-CaMP2 fluorescence was reflected off a 585-nm dichroic (Chroma, T585LP) and passed through a 630-75–nm emission filter (Chroma, ET630/75m). Images were acquired at 10 Hz using QCapture Pro7 Software (Q-imaging). During synchronous measurement of GCaMP6m or R-CaMP2 fluorescence from

a neuron, action potentials were driven by brief current pulses (5 ms, 1–2 nA) injected at 10 Hz for 3 s (resulting in 30 action potentials). We defined the response size to the stimulation train as the difference between the mean stimulus dF/F during the first 3 s of the stimulation train and the mean baseline dF/F during the 3 s before the stimulation train.

bReaChES design and characterization. bReaChES was generated by introducing a Glu123Ser mutation and replacing the first 51 amino-terminal residues with the first 11 amino-terminal residues of channelrhodospin 2 in the previously published ReaChR construct[21,22]. Dissociated rat hippocampal neurons were cultured and transfected with either ReaChR or bReaChES. The same intracellular recording procedures were used as for the GECI isosbestic cultured neuron intracellular recordings. Action potentials were elicited with a 4-s pulse train of 590-nm light (5-ms pulse width) delivered at various frequencies using a Spectra X Light source and 590-10–nm excitation filter (Thorlabs). Steady-state current and tau-off kinetics were measured using a constant illumination of 4 s.

Animal surgical procedures and viruses. All experimental and surgical protocols were approved by Stanford University's Institutional Animal Care and Use Committee. For all surgeries, stainless steel head plates and ferrules were fixed to the skull using Metabond (Parkell). For all experiments, we used DAT∷Cre B6.SJL-*Slc6a3tm1.1(cre)Bkmn*/J (JAX stock 006660) female or male transgenic mice aged 6–8 weeks. No experimental differences due to gender were observed. Mice were anesthetized with 1.5–2.0% isoflurane and placed on a heating pad in a stereotaxic apparatus (Kopf Instruments). All viruses were produced at the Stanford Viral and Vector Core–GVVC (Stanford University).

For the seven-fiber surgery, four mice were stereotaxically injected as previously described[13] with 500 nL of AAVDJ-CaMKIIα-GCaMP6f (2.7e12 vg/ml) at six locations: PFC, anterior-posterior (A/P) +2.2, medial-lateral (M/L) +0.35, dorsal-ventral (D/V) −2.2; NAc, A/P +1.15, M/L −1.65, D/V −4.2; BLA, A/P −1.54, M/L −3.0, D/V −4.6; lateral hypothalamus, A/P −0.9, A/P −1.1, D/V −5.0; bed nucleus of the stria terminalis, A/P +0.9, M/L +0.1, D/V −4.4; and CA1, A/P −1.75, M/L +1.5, D/V −1.25. Mice were injected with 1,000 nL of AAVDJ-EF1α-DIO-GCaMP6f (1.5e13 vg/ml) in the VTA (A/P −3.1, M/L −0.4, D/V −4.4). Custom 400-μm-diameter, 0.48-NA fibers attached to a 1.25-mm-diameter stainless steel ferrule (Doric Lenses) were stereotaxically implanted at the same seven coordinates.

For four-fiber surgeries, seven mice were injected with 1,000 nL of AAVDJ-EF1α-DIO-GCaMP6f (1.5e13 vg/ml) at two locations in the VTA: A/P −3.3, M/L −0.3; and M/L −0.5, D/V −4.2. Custom 400-μm-diameter, 0.48-NA fibers attached to a 1.25-mm-diameter stainless steel ferrule were stereotaxically implanted at four locations: VTA, A/P −3.3, M/L −0.4, D/V −4.2; PFC, A/P +2.2, M/L −0.35, D/V −2.0; NAc, A/P +1.2, M/L −1.75, D/V −4.0; and BLA, A/P −1.54, M/L −2.8, D/V −4.5. Two mice from this surgery cohort were also used for the simultaneous camera and photoreceiver comparison experiment.

For dual-color R-CaMP2 and GCaMP6 imaging, a single mouse was injected with 1,000 nL of a 1:1 mixture of AAVDJ-hSyn-DO-GCaMP6m (2.9e12 vg/ml) and AAVDJ-EF1α-DIO-RCaMP2 (8.0e12 vg/ml) in the VTA at A/P −3.3, M/L −0.4, D/V −4.2. A custom 400-μm-diameter, 0.48-NA fiber attached to a 1.25-mm-diameter stainless steel ferrule was implanted at the same location.

For GCaMP6 imaging and bReaChES stimulation, a single mouse was injected with 1,000 nL of a 1:1 mixture of AAVDJ-EF1α-DIO-GCaMP6f (1.5e13 vg/ml) and AAVDJ-EF1α-DIO-bReaChES-TS-mCherry (5.8e12 vg/ml) in the VTA at A/P −3.3, M/L −0.4, D/V −4.2. A custom 400-μm-diameter, 0.48-NA fiber attached to a 1.25-mm-diameter stainless steel ferrule was implanted at the same location. As a control, a single DAT∷Cre mouse was injected with 1,000 nL of a 1:1 mixture of AAVDJ-EF1α-DIO-GCaMP6f (5.8e12 vg/ml) and AAV8-EF1α-DIO-mCherry (1.7e13 vg/ml) in the VTA and implanted with a 400-μm-diameter, 0.48-NA fiber at the same coordinates as in the experimental mouse.

Histology. Mice were heavily anesthetized with isoflurane and then perfused with 20 mL of cold phosphate-buffered saline (PBS) followed by 20 mL of cold paraformaldehyde. The brain was extracted from the skull, kept in paraformaldehyde for 24 h and then transferred to a 30% sucrose solution. After 48 h, the brains were sliced into sections 50–100 μm thick using a vibratome (Leica VT1200S) in cold PBS. Slices were then washed in PBS at room temperature three times for 5 min each. For GCaMP6 and tyrosine hydroxylase (TH) staining, slices were incubated in a blocking solution of PBS + 0.3% Triton-X (PBST) with 5% normal donkey serum (NDS) for 1 h. Slices were then incubated for 24 h at 4 °C in PBST + NDS blocking solution containing a primary rabbit antibody to GFP conjugated to Alexa Fluor 488 (Life Technologies, A21311, 1:500) and a primary chicken antibody to TH (Aves Lab, TYH, 1:500) (ref. 13). Slices were washed three times for 10 min each time in PBST and then incubated in blocking solution containing secondary donkey anti-chicken conjugated to Alexa Fluor 647 (Millipore, AP194SA6) for 2 h at room temperature. Slices were washed with PBST three times for 10 min each time and finally stained for DAPI (1:1,000) for 10 min and mounted onto glass slides. For the TH staining in the dual-color mouse, normal goat serum was used instead of NDS, and no Triton-X was added at any step. The same TH antibody was used with secondary goat anti-chicken conjugated to Alexa Fluor 647 (Life Technologies, A21449, 1:500). No DAPI or primary antibodies to GCaMP6 or R-CaMP2 were used.

21. Lin, J.Y., Knutsen, P.M., Muller, A., Kleinfeld, D. & Tsien, R.Y. *Nat. Neurosci.* **16**, 1499–1508 (2013).
22. Rajasethupathy, P. *et al. Nature* **526**, 653–659 (2015).